Journal of Clouds, Aerosols and Radiation
J. Clouds, Aerosols & Rad. (2014) 1, 1—17

Sensitivity of the Warm Rain Process in Convective Clouds to Regional Climate Change in the Contiguous U.S.

C. M. Villanueva-Birriel[1], S. Lasher-Trapp[1], R. J. Trapp[1], and N. S. Diffenbaugh[1,2]

[1]*Department of Earth, Atmospheric and Planetary Sciences, Purdue University*
550 Stadium Mall Drive, West Lafayette, IN 47907, USA

[2]*Dept. of Environmental Earth System Science & Woods Institute for the Environment, Stanford University,*
Jerry Yang & Akiko Yamazaki Environment & Energy Building, 473 Via Ortega, Stanford, CA 94305

(Submitted 16 Sept. 2013; Accepted 11 Dec. 2013; Revised 2 Feb. 2014; Published 16 May 2014)

ABSTRACT

The hypothesis of an increase of the warm rain process within deep convective clouds under anthropogenic climate change is tested. A 1D warm rain microphysical model that represents the core of the clouds is run with past and future thermodynamic profiles derived from a global climate model and local aerosol estimates. The depth from the cloud base to the freezing level increases substantially in the future clouds. However, an arid environment, a faster updraft speed, or higher amounts of cloud condensation nuclei (CCN) can offset this effect, diminishing or preventing the expected increase in warm rain formation. The future clouds in some regions also exhibit a decreased sensitivity to CCN. These experiments illustrate that a universal assumption of a more active warm rain process in a warmer future climate is inappropriate. Future precipitation enhancement is likely to occur in regions where the warm rain process is currently marginally productive.

Corresponding author address: C. M. Villanueva-Birriel, E-mail: cvillanu@purdue.edu.
Keywords: warm rain process, convective clouds, precipitation, climate.
Citation: Villanueva-Birriel, C. M., Lasher-Trapp S., Trapp R. J., and Diffenbaugh, N. S. (2013). Sensitivity of the Warm Rain Process in Convective Clouds to Regional Climate Change in the Contiguous U.S. *J. Clouds, Aerosols & Rad.*, 1**,** 1–17.

1. Introduction and Motivation

Throughout the twentieth century, precipitation has increased by 10 % in the contiguous U.S., reflected mainly in the heavy and extreme daily precipitation events, at the expense of more moderate events (Karl and Knight, 1998), and this increase is more prominent during the summer months of the year. Other studies have similar findings regarding the increase in extreme events around the globe (Allan and Soden, 2008; Lau and Wu, 2007, 2011). Berg et al. (2013) concluded that convective precipitation is more sensitive to increasing temperatures than stratiform precipitation, influencing extreme precipitation events more. These findings suggest potentially higher occurrences of flooding that could significantly impact numerous aspects of life and society. However, the details of how exactly precipitation formation within convective clouds in these heavy and extreme events changes with rising temperatures are lacking in these statistical studies.

The cloud lifetime and production of precipitation within deep convective clouds involves a complex interplay between different microphysical processes, the cloud dynamics, and large-scale environment. The microphysical processes include activation of cloud condensation nuclei (CCN) and growth by condensation, further growth by collision-coalescence (the so-called "warm rain process," up to this point), continuing to the nucleation of ice particles upon ice nuclei, either from the vapor or freezing of cloud or raindrops that may then quickly grow by riming to form graupel (or even hail), which often melt upon descent beneath the freezing level to fall to the ground as rain. The transport of and interaction among this myriad of microphysical particles through the cloud depends upon the larger-scale dynamics of the cloud (e.g. updrafts and downdrafts), as well as how large the particles grow before falling from the cloud. Ultimately, the cloud lifetime controls the amount of precipitation produced, as it determines at what point the microphysical processes terminate (i.e. conversion of water vapor to liquid or ice), as well as the updrafts needed to suspend the particles in their regions of growth.

There has been evidence in the past that some of the heaviest convective rainfall events may be due to an extremely productive warm rain process. Such evidence has usually consisted of identifying radar reflectivity maxima consistently at or beneath the freezing level. Such features are common in tropical storms (e.g. Houze, 1977; Maheshwari and Mathur, 1968) but are even possible over continental regions where droplet concentrations are higher and the warm rain process might be assumed to be less productive. Caracena et al. (1979) identified such a radar signature in the data from the Big Thompson Flood, and a summary of extreme rainfall events by Baeck and Smith (1998) also identified this radar signature (and implicated a strong warm rain process) in Virginia, Texas, and North Carolina. Peterson et al. (1999) similarly discussed the likelihood of a strong warm rain process in the Fort Collins flash flood, and Golding et al. (2005) presented evidence for a strong warm rain process in the Boscastle, England flood. It has often been argued that continued global warming should cause the warm rain process (WRP) to be more productive given a greater depth over which it can act in a warmer troposphere, and if so this might be indicative of the potential for more frequent extreme convective rainfall events.

As a first step in investigating such a scenario, this study uses a full atmosphere-ocean GCM to supply plausible thermodynamic environments in which deep convective clouds grow in the contiguous U.S. during the summer months. A detailed microphysical parcel model is initialized with those atmospheric profiles and estimates of local aerosol, to evaluate the response of the WRP due to regional climate change. By comparing the precipitation formed by the WRP in past and future simulated climates, the results can be used to interpret precipitation responses in observational studies or in more complex dynamical models that must necessarily sacrifice details in their microphysical representation. The results are not meant as predictions of the locations of future extreme precipitation events, as ice processes,

storm structure and evolution, and even storm initiation are not investigated here. Moreover, the thermodynamic environments used here are based upon a single run of one GCM. Rather, this initial study is an idealized study, using thermodynamically plausible environmental changes provided by the GCM output. These results can then provide guidance for establishing expected trends for regions with similar thermodynamic and aerosol conditions to those represented here, helping to identify where the WRP might be expected to be the most affected by future climate change not only in the U.S, but also in similar environments worldwide.

2. Changes in Thermodynamic Environment and Effects on Cloud Structure

Probing the response of convective precipitation can be accomplished by running simulations of the atmospheric environment during periods of high convective available potential energy (CAPE), using sub-daily, 3D output (e.g., Trapp et al., 2007). Here one of the NCAR CCSM3 simulations described in Trapp et al. (2009) is used to represent the period from 1950 to 2099 in the SRES A1B scenario. Vertical environmental profiles of atmospheric temperature, pressure, moisture, and wind were averaged from instances when simulated CAPE[1] exceeded 1000 J kg^{-1} at 00 UTC during the summer months (June, July, August) of the 1970-1999 and 2070-2099 ("past" and "future") periods, respectively. The CCSM3 3D model output occurs every 6 hours; during the summer, strong late afternoon and evening maxima of precipitation are observed in most of the U.S. (Trenberth et al., 2003), so the 00 UTC output was used as the environmental conditions for the simulations. Trapp et al. (2007) also chose to use the 00 UTC output, because they found it represented the typical time of maximum CAPE, as confirmed by computing CAPE at the other CCSM3 output times. Sixty-one different sites across the U.S. (Table 1) were selected to investigate rural, urban, and coastal regions. The CCN parameters "C" and "k" are constants of the CCN activity distribution described in Section 3.1 and were taken as best estimates from the literature, but do not purport to be representative of all extremes possible at a given location. The use of two average soundings to represent the "past" and "future" environments does eliminate some potential variability at a given site, but is appropriate to evaluate the mean climatological response sought here.

The number of profiles (and hence days) exceeding the CAPE threshold for each site (Fig. 1) illustrate that in this particular climate simulation, the Great Plains and Southeast are preferred regions for deep convection, in accord with past work using observations and reanalysis data (e.g. Brooks et al., 2003). In the future climate scenario, these preferred regions have even greater frequencies of large CAPE (Fig. 1b), and expand, particularly northward (Fig. 1c).

The averaged vertical profiles are warmer throughout the depth of the troposphere in the future climate. A typical profile (Fig. 1, inset) shows temperatures increase by several degrees Celsius; dewpoint temperatures are more variable among the sites, but may increase by one or more degrees Celsius. The averaged profiles exhibit a relatively dry layer below the 700 hPa height at nearly all locations. Comparisons conducted with 30-year averages of North American Regional Reanalysis (NARR; Mesinger et al., 2006) data and 20-year averages of NCEP-NCAR Reanalysis Project (NNRP; Kalnay et al., 1996) data confirmed a dry bias in the CCSM3 simulations. The dry boundary layer in these profiles increases the estimated height of the cloud bases; however, because differences between past and future climates are being emphasized here, it is not a major detriment to the outcomes of this study.

Table 1: Sites and CCN conditions for which the microphysical model was run.

[1] Trapp et al. (2007 and 2009) looked at CAPE thresholds of 100 or 2000 J/kg and found similar trends to those in this paper. Additionally, the threshold used here was appropriate for finding strong storms with a reasonable amount of cases included in the average profiles.

Location	Longitude	Latitude	CCN: C (cm^{-3})	CCN: k
Seattle, WA	-122.33	47.61	1200	0.7
Klamath Falls, OR	-121.78	42.22	600	0.4
Sunnyside, WA	-120.01	46.32	600	0.5
Carson City, NV	-119.75	39.16	600	0.7
San Diego, CA	-117.15	32.78	1200	0.7
Las Vegas, NV	-115.14	36.18	900	1.2
Jerome, ID	-114.52	42.72	600	0.5
Cedar City, UT	-113.07	37.68	700	0.8
Phoenix, AZ	-112.07	33.45	900	1.2
Salt Lake City, UT	-111.89	40.76	900	1.2
Bozeman, MT	-111.05	45.68	700	0.8
Winslow, AZ	-110.7	35.02	600	0.5
Jackson, WY	-110.67	43.61	600	0.5
Vernal, UT	-109.53	40.46	600	0.5
Billings, MT	-108.54	45.79	900	0.8
Durango, CO	-107.88	37.28	600	0.6
Santa Fe, NM	-105.94	35.69	900	1.2
Pueblo, CO	-104.61	38.25	900	0.8
Roswell, NM	-104.52	33.39	600	0.5
Alpine, TX	-103.67	30.36	700	0.8
Scottsbluff, NE	-103.66	41.87	600	0.5
Rapid City, SD	-103.23	44.08	600	0.7
Dickinson, ND	-102.79	46.88	700	0.8
Amarillo, TX	-101.83	35.22	3000	0.8
Jamestown, ND	-98.7	46.91	600	0.7
San Antonio, TX	-98.5	29.42	3000	0.8
Salina, KS	-97.61	38.84	600	0.5
Oklahoma City, OK	-97.52	35.47	900	1.2
Watertown, SD	-97.11	44.9	900	1.2
Dallas, TX	-96.8	32.78	4000	0.8
Tulsa, OK	-95.99	36.15	900	1.2
Omaha, NE	-95.94	41.26	900	1.2
Houston, TX	-95.38	29.76	3000	0.8
Rochester, MN	-92.47	44.02	900	1.2
Columbia, MO	-92.33	38.95	600	0.5
Vicksburg, MS	-90.88	32.34	600	0.5
New Orleans, LA	-90.08	29.95	400	0.5
Springfield, IL	-89.64	39.8	900	1.2
Madison, WI	-89.4	43.07	1000	0.7
Jackson, TN	-88.82	35.63	600	0.5
Chicago, IL	-87.65	41.85	650	0.6
Pensacola, FL	-87.22	30.42	400	0.5
Jasper, IN	-86.93	38.39	700	0.7
Birmingham, AL	-86.81	33.52	1200	0.9
Dayton, OH	-84.19	39.76	1800	0.7
Saginaw, MI	-83.95	43.42	600	0.5
Knoxville, TN	-83.94	35.97	1200	0.9
Douglas, GA	-82.85	31.51	600	0.5
Anderson, SC	-82.65	34.51	800	0.7
Orlando, FL	-81.38	28.54	700	0.7
Charlotte, NC	-80.84	35.23	1400	0.9

Miami, FL	-80.22	25.79	800	0.7
Pittsburgh, PA	-79.996	40.44	700	0.7
Charleston, SC	-79.93	32.78	800	0.6
Elkins, WV	-79.85	38.92	600	0.5
Jacksonville, NC	-77.41	34.76	700	0.6
Syracuse, NY	-76.14	43.05	1000	0.8
Philadelphia, PA	-75.17	39.95	2000	1.0
New York City, NY	-74.01	40.71	1300	0.7
Providence, RI	-71.41	41.82	400	0.4
Greenville, ME	-69.59	45.46	400	0.4

Because the WRP starts at the cloud base and depends upon the cloud liquid water content, it is informative to first consider how the cloud base conditions differ across the U.S., and between the past and future environments. The vertical thermodynamic profile determines the cloud base (estimated by the lifting condensation level) and the adiabatic liquid water content (the maximum amount of condensate achieved at any height above cloud base), and thus can be compared for the past and future profiles derived from the CCSM3 simulations. The cloud base temperature is generally greater in the eastern half of the U.S. both due to the moister boundary layer air there and the lower elevation, and is maximized in the Southeastern U.S. (Fig. 2a). That trend does not change in the future climate scenario (Fig. 2b), but all future cloud bases occur at greater temperatures (Fig. 2c), especially in the Midwest, and due to increased moisture, they are also about 200 m lower in altitude. Lower, warmer cloud bases favor the WRP by allowing fewer droplets to be nucleated [drops grow more quickly by condensation, limiting the maximum supersaturation achieved above cloud base for CCN activation (Johnson, 1980)], promoting faster droplet growth by condensation and quicker onset of collision-coalescence. These lower, warmer cloud bases combine with a higher freezing level (FL) to increase the adiabatic liquid water content at the future FL (Fig. 2 d-f), especially in the Midwest (Fig. 2f). The aridity of the West, despite increasing temperatures, in general continues to limit cloud base heights and adiabatic liquid water content there, with some exceptions[2].

The cloud depth to the FL provides another estimate of the potential productivity of the WRP, and is often argued as justification for assuming warm rain will be more prevalent as the climate warms (e.g. Lindzen et al., 2001; Freud and Rosenfeld, 2012; Konwar et al., 2012). The greatest depths in the past have occurred along the Gulf Coast and Florida (Fig. 3a), sometimes exceeding 4500 m, but only range from 1500-3000 m in the Western U.S. In the future scenario, the large values previously seen over the Gulf Coast extend to the northern U.S. border in much of the East and Midwest (Fig. 3b), yielding increases exceeding 800 m at some sites (Fig. 3c). Such increases are due in part to the lower future cloud bases in this region, and also to an increase in the mean freezing level height over these regions due to an overall warmer troposphere predicted by the climate model. Although all regions have a greater cloud depth to the FL in the future, arid regions with high cloud bases like those in the West still have depths less than 3000 m, which will be shown in the results presented later, to limit the WRP due to the lower probability to attain an efficient coalescence process that could increase precipitation amount within the cloud, also noted by Freud and Rosenfeld, (2012). The South, where depths exceeded 4000 m in the past, show some substantial increases in the future, but regions that had moderate values in the past (the East and Midwest) exhibit the greatest increases in the future.

[2] A few Western sites had significantly more moisture at the lowest level in the future, creating anomalies of lower and warmer cloud bases, and thus higher adiabatic liquid water contents.

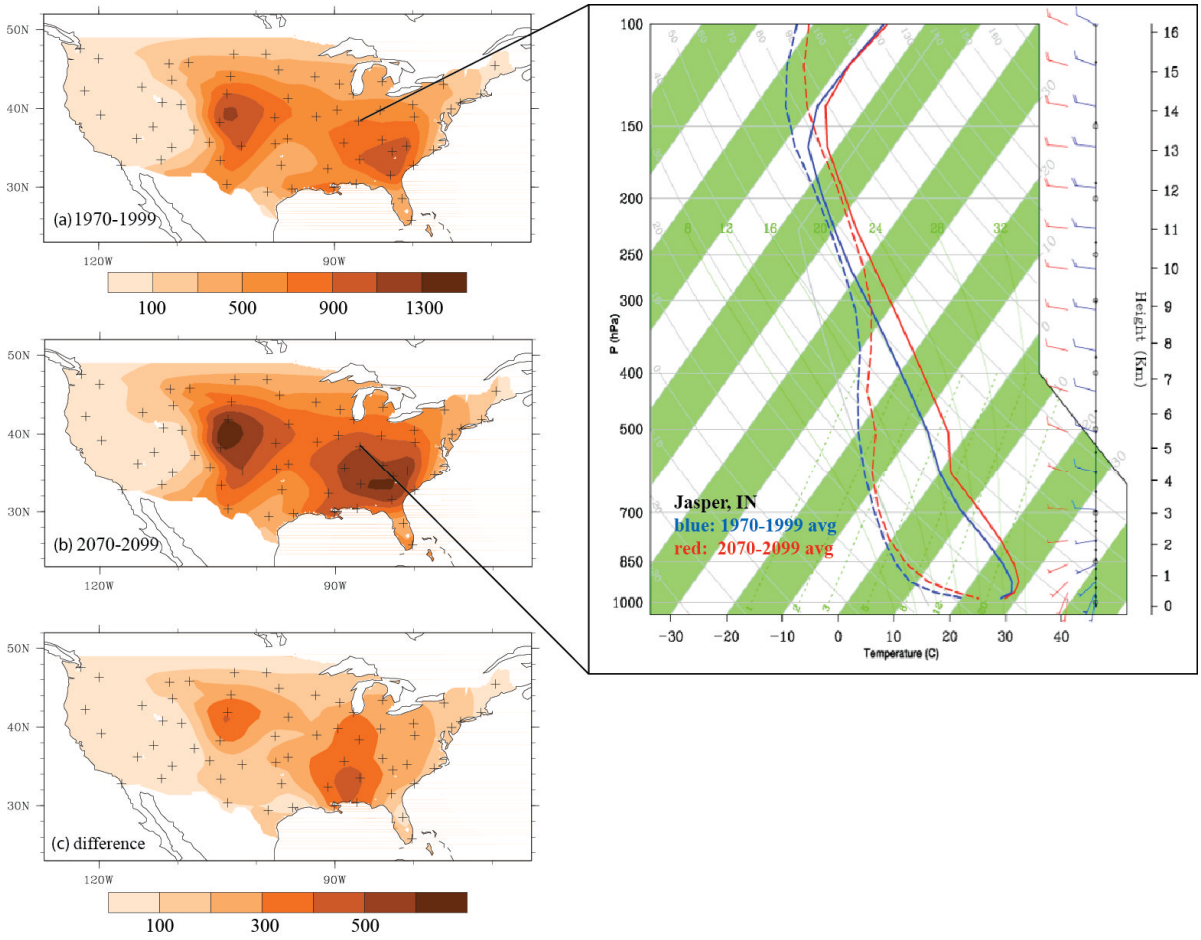

Fig. 1. Number of 00 UTC vertical thermodynamic profiles from the CCSM3 results per 30-year period that exceed 1000 J kg^{-1} in CAPE and thus contributing toward the 30-year average, at sites marked by crosses for (a) 1970-1999, (b) 2070-2099, and (c) difference in (b) and (a). Top color bar for (a) and (b); bottom color bar for (c). Inset: example of averaged vertical profiles plotted on skew-T chart for Jasper IN, for 1970-1999 (blue) and 2070-2099 (red).

However, the updraft speeds also increased from the past to the future at all sites (Fig. 3 d-f) by as much as 3 m/s. The updraft speed here is only a function of the parcel buoyancy integrated up to the FL[3], so greater CAPE values yield greater updraft speeds in this analysis and the model calculations presented in the next section, and should be considered maximum updraft speeds in the core of the storms where entrainment has been limited.

Thus the increased depths to the FL (Fig. 3 a-c) are partially offset by updraft speed increases, modulating the time an air parcel travels from cloud base to the FL, and thus the time over which collision-coalescence can act to form raindrops (Fig. 3 g-i). The regional patterns seen in the cloud depth to the FL (Fig. 3c) do not always coincide with the parcel ascent time to the FL (Fig. 3i), demonstrating that a greater cloud depth to the FL does not easily scale to increased time for warm rain production. Areas with future cloud depth increases must have only minor or no increases in updraft speed in order to enhance the WRP. In this particular climate simulation, the Midwest is especially favored in this regard. Calculations of the microphysical details of the WRP to further evaluate and understand these trends are presented in the next section.

[3] Updraft speeds were calculated from the 1D model described in the next section.

3. Microphysical Modeling

The 1D Lagrangian bin-resolving warm rain model of Cooper et al. (1997) was used to calculate the progression of the WRP in the past and future clouds grown in the environments presented in the previous section. The model makes detailed microphysical calculations such as simultaneous condensation and quasi-coalescence of a droplet population within a closed air parcel ascending adiabatically. The model has been adapted here to push the parcel through any negative buoyancy near cloud base up to the level of free convection; the updraft velocity above this level is calculated from the buoyancy of the parcel relative to its environment and neglects any effects of entrainment. In this sense, it is representative of the microphysics occurring in the core of the storm. The core of a convective cloud is mainly driven by strong updrafts. Heymsfield et al. (1978) and Musil et al. (1986) found undiluted cores within the main updraft of deep convective clouds with nearly adiabatic liquid water content, especially close to cloud base, and updraft speeds close to those calculated by parcel theory have also been documented (Bluestein el al. 1988). Hence, entrainment effects should be minimal in the precipitation development within the cores of the storms modeled here. Twomey (1976) showed that regions of high liquid water content were critical for growth of precipitation particles due to the rapid evolution of large droplets, which can also enhance the ice particle and hailstone growth rates (not represented in the 1D model used here) and consequently, precipitation reaching the ground. Thus, this model is suitable to understand key differences in the initial stages of the WRP between past and future environments, and possible effects upon ice processes aloft and subsequent precipitation are discussed in the last section.

3.1 Warm rain process in microphysical model

The 1D Lagrangian microphysical model is that of Cooper et al. (1997), initialized for each site at cloud base using the conditions found from the averaged vertical profile and ascends adiabatically as if within the cloud core up to the FL. The incremental changes in pressure during parcel ascent are calculated from the vertical wind and hydrostatic equation. The vertical wind is obtained from the parcel buoyancy. Vertical displacement of the parcel is evaluated by simply multiplying the vertical wind by the current time step.

At the start of the model run, 512 logarithmically-spaced bins are initialized for sizes ranging from 0.01 μm to 1 cm to represent the aerosol size distribution. This distribution is represented in three parts. The small sizes in the distribution ($r < 0.1\mu m$) are characterized by a cloud condensation nuclei (CCN) activity distribution $N = C(S/S_o)^k$ where N is the cumulative number of CCN activated at or below supersaturation S, S_o is a reference supersaturation (generally 1%) where $N(S_o)$ equals C, and k is a constant. C and k will vary depending on the type of environment (e.g. continental or maritime). A Junge distribution (Junge et al., 1969) is assumed for the intermediate sizes (0.1-1.0 μm) at supersaturations 0.007 % to 0.4 %, and giant CCN (> 1.0 μm) are characterized by a power law relation (see Cooper et al., 1997 for more details). CCN observations at most sites listed in Table 1 were not available in the literature, and so a compilation of CCN measurements by Pruppacher and Klett (1997), augmented by measurements found in the literature (Twomey and Wojciechowski, 1969; Braham, 1974; Spyers-Duran, 1974; Auer, 1975; Hobbs et al., 1978; Hobbs et al., 1985; Frisbie and Hudson, 1993; Hudson and Yum, 2001; Lasher-Trapp et al., 2008), were used to identify regions with similar (urban, rural, coastal) characteristics. Values of C (the number of CCN activated at 1% supersaturation) range from 300 in coastal areas

(influenced by cleaner air from over the ocean) to over 4000 cm^{-3} at some urban sites[4] were used to test for a variety of responses in the WRP to regional climate change.

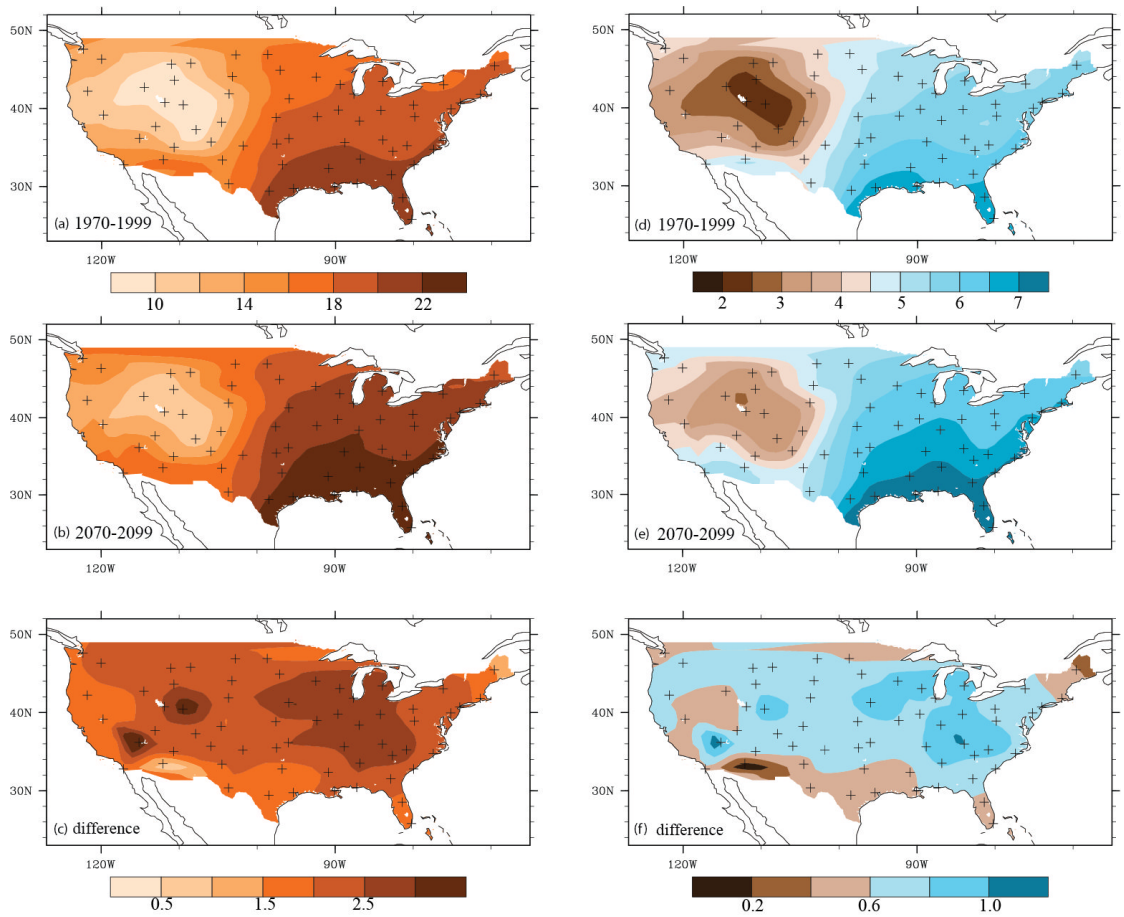

Fig. 2. As in Fig. 1., except cloud base temperature in °C (left) and adiabatic liquid water content at the height of the freezing level in g m^{-3} (right) for the past (a,d) and future (b,e) environments, with scales as noted. Differences (b-a, or e-d) shown in (c,f) on different scale beneath the plot.

As the parcel ascends and cools, the supersaturation increases and CCN start to activate. Once CCN are activated, the condensational growth rate of each bin is calculated at each time step; all droplets in each bin grow at the same rate. This method avoids reassignment of droplets to other bins done in other parcel models that could artificially broaden the droplet size distribution. The Fukuta-Walter equation (Eq. B1 in Cooper et al., 1997) was used for the implementation of condensational growth within the model, taking into account the transfer of heat energy between water vapor and liquid molecules across the water interface of the droplet, and the fraction of impinging water vapor molecules that is actually retained by the water surface in the droplet. These kinetic effects are especially important for small or newly nucleated droplets or for particles that remain small for a long period of time. Without these effects, the mass of droplets growing in the first 20 s would be twice as large compared with droplets in the case with these effects taken into account (Fukuta and Walter, 1970). As increasingly more CCN are activated, eventually the supersaturation reaches a maximum in the parcel, and the maximum cloud droplet number concentration is attained, whereupon the supersaturation decreases with additional parcel ascent as the droplets grow.

[4] For some sites, extreme examples found in the literature were used to investigate the responses in the WRP, and might not be representative of the average daily CCN at that site.

The quasi-stochastic collision and coalescence approach was implemented in the model using a modified Kovetz and Olund (1969) scheme. In this scheme a coalesced drop is assigned to the appropriate bin nearest to the correct size, but the average size assigned to that bin is modified to conserve mass. This modification, implemented by Cooper et al. (1997), was necessary to avoid numerical broadening of the size distribution due to the acceleration of the growth of the largest drops. Thus, the adjustment improves the representation of large drops growing by collecting smaller cloud drops. The calculated collection efficiencies from Cooper et al. (1997, Fig B1), which depends on the collector and collected drop radii, were used in the model to represent the fraction of collision-coalescence events.

Drop breakup due to drop collisions was not included in the calculations; instead drops in collision events with no coalescence maintained their initial drop sizes. However, since in the initial stages of precipitation production in the WRP, most collisions are between growing collector drops and cloud droplets, this assumption is not severely restrictive. To avoid unrealistically large drops as coalescence progressed, a simple drop breakup representation was implemented where the number of drops larger than 6 mm was assumed to decrease exponentially with a time constant of 10 s, and the mass from these larger drops was reinserted at the 6 mm size bin, as in Cooper et al. (1997). Raindrop sedimentation is not represented in the 1D Lagrangian model, but it is not important here, as updraft speeds in convective storms are typically much greater than the fall speeds of the largest raindrops.

An adaptive time-step employing a Runge-Kutta scheme was used for the growth of each droplet. The Runge-Kutta scheme was evaluated to the fourth or fifth order for the droplet growth with varying time step sizes depending on the microphysical process involved (See Cooper et al., 1997 for more details). The model automatically calculates time steps and were on the order of 0.001-0.1 s in the initial stages of the calculations where condensation was more prominent, and then increased to 1-5 s for coalescence events as needed for numerical stability (Cash and Karp 1990).

3.2 Warm rain production at the freezing level

The microphysical model outputs a complete droplet size distribution at a regular height interval, so the amount of raindrop production can be quantified at the FL, as a gauge of the productivity of the WRP. For the discussion below, any drops greater than 100 μm radius are considered as raindrops or as contributing to the precipitation water content.

The variability in cloud droplet number concentration at 100 m above cloud base (Fig. 4a) is largely a function of the number of CCN initialized in the model at each site. Urban sites are clearly evident in Texas, the Midwest, and in the Northeast, with lower values occurring in rural regions, and the lowest values occurring near coastlines. The number of cloud droplets at each site decreases in the future as expected from the warmer cloud bases, but the largest changes occur at the urban sites (Fig. 4c). The amount of condensate converted to raindrops (here designated as having radius exceeding 100 μm) increases in the future (Fig. 4a and b), in some cases by more than 20%. An example of drop size distributions (Fig. 5) at 100 m above the cloud base, where the maximum droplet concentration is usually found in the cloud, and at the FL show the more numerous, larger raindrops that can be produced in the future environment. The increased precipitation mass results from larger raindrops at the FL that is due to the longer time that collision-coalescence can act. The greatest regional increases occur in the Dakotas and Midwest (Fig. 4f), but interestingly, some of the greatest increases in precipitation mass also occur at urban sites (explored in the next section).

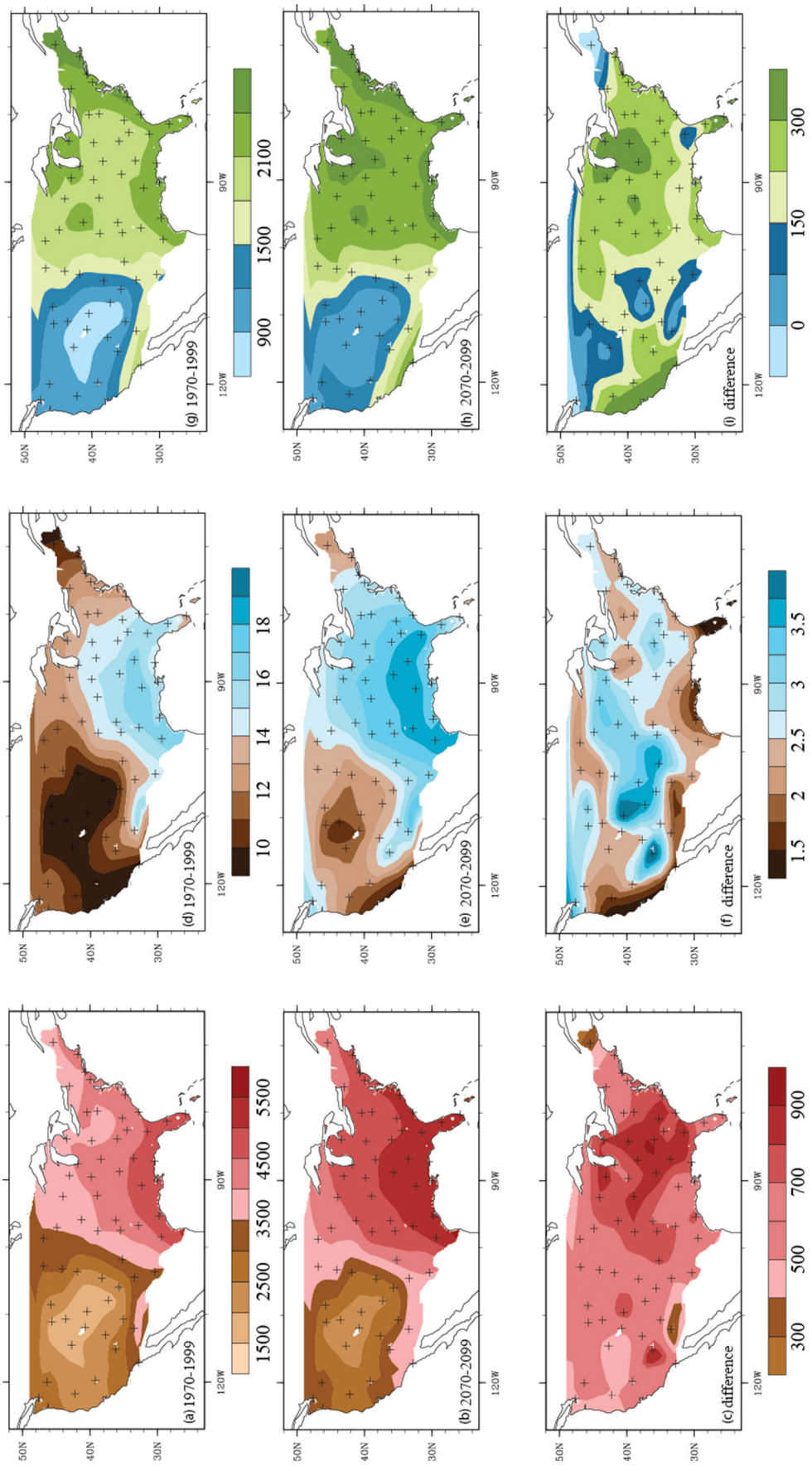

Fig. 3. As in Fig. 1, but here depth from cloud base to the freezing level in m (a,b), updraft speed at the freezing level in m s^{-1} (d,e), and parcel ascent time between cloud base and the freezing level in s (g,h) for the past (top row) and future (middle row) atmospheric profiles at the 61 sites for which the microphysical model was run (crosses), with scales shown. Differences between past and future results (b-a), (e-d) or (h-g) are shown in (c, f, i), respectively, on different scales beneath the plots.

3.3 Decreased sensitivity to CCN

It has long been established that the productivity of the WRP is a strong function of the CCN in the ambient environment that is ingested by the cloud. More CCN result in smaller droplet sizes that can delay (or even preventing) the onset of collision-coalescence and generation of raindrops. If all other factors are favorable for the WRP (warm, low cloud bases and a high FL) but too many CCN are present, then warm rain production can be prevented. On the other hand, if all other factors are quite favorable for the warm rain process, then more CCN do not necessarily halt warm rain formation. Thus, the number of CCN required to limit/prevent warm rain formation is a function of how favorable those other factors are. Some larger-scale modeling studies with parameterized microphysics have suggested a decreased sensitivity of precipitation production in storms forming in warmer climates to increased numbers of CCN; Storer et al. (2010), for example, used a cloud resolving model and found that more unstable environments suppressed the CCN limitations on precipitation, while CCN played a major role in modulating precipitation in the storms occurring in more stable environments.

The microphysical model was re-run twice at all sites for the past and future thermodynamic profiles, initialized identically with C = 700 or 2000 cm^{-3}, representative of continental and polluted environments, respectively, regardless of location[5]. Figure 6 shows the percent change in precipitation mass with this increase in CCN concentration. For most locations, precipitation mass decreased when the CCN concentration increased, in the past environment and in the future one (Fig. 6 a and b, indicated by the negative change). The most sensitive cases in the past (Fig. 6a) occurred in the West, where some sites had "marginally" favorable environments for warm rain production if fewer CCN were present, but no warm rain was produced when CCN were too numerous[6]. The East showed little sensitivity to changes in CCN in the past (Fig. 6a), but several sites exhibited a *decreased* sensitivity to CCN in the future (Fig. 6b), particularly those in the Dakotas and in the Texas Panhandle, where the future environments are so favorable for warm rain production. A significant part of the Midwest shows no sensitivity to CCN in the future, resulting from the very favorable environment there for warm rain production, as discussed in Section 2. A few sites in the Southwest have an increased sensitivity to CCN in the future, because their past environments were unfavorable for the WRP regardless of CCN amount, but their future environments can potentially allow some warm rain, if CCN are not too numerous. If the thermodynamic conditions derived from the climate model results are verified in the future, this would suggest some relief to arid regions, but this warrants further study considering the potential for storm initiation and a more thorough representation of the storm dynamics and ice processes.

[5] The model was also run twice more for several sites changing the slope of the CCN distribution input into the model (k) from 0.2 to 1.5, representative of changing the aerosol chemical composition and thus reducing the cumulative activated CCN concentration for S < 1%. Although not presented here, the CCN sensitivity results were much less than when C was changed.

[6] Runs with more giant aerosols (not shown), if accompanying more CCN, were capable of producing limited amounts of rain (but less than those cases with fewer CCN).

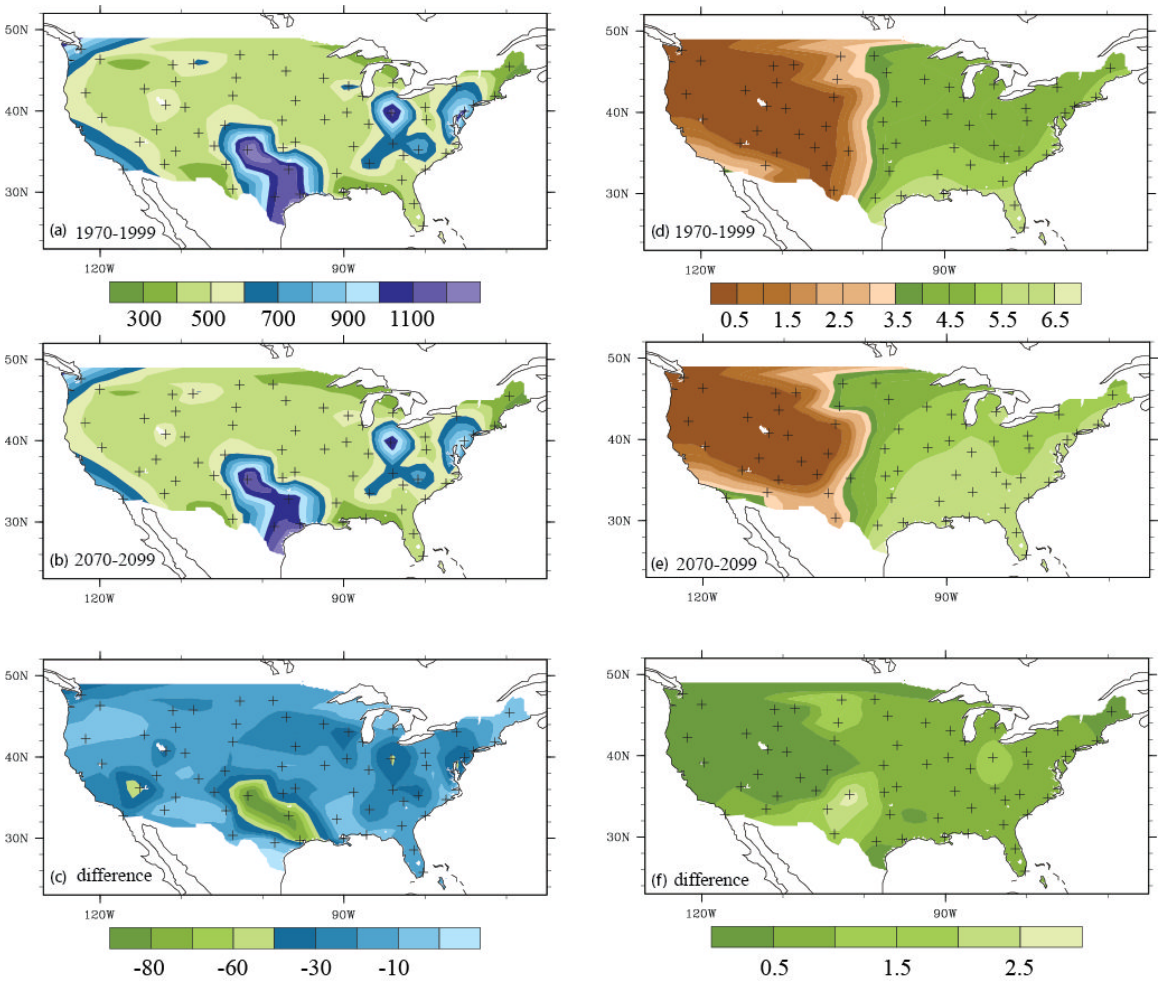

Fig. 4. As in Fig. 1, except number of cloud droplets per cm^{-3} near cloud base (a, b) and precipitation water content in g m^{-3} at the freezing level (d,e), with differences shown in (c) and (f).

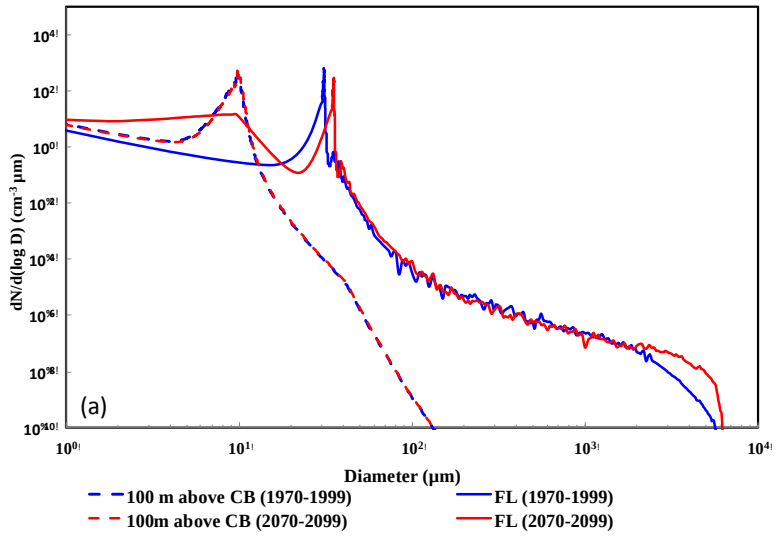

Fig. 5. Drop size distributions produced by the 1D model for Alpine, TX for past (blue) and future (red) environments. Size distributions at 100 m above cloud base denoted by dashed lines, and at the FL by solid lines.

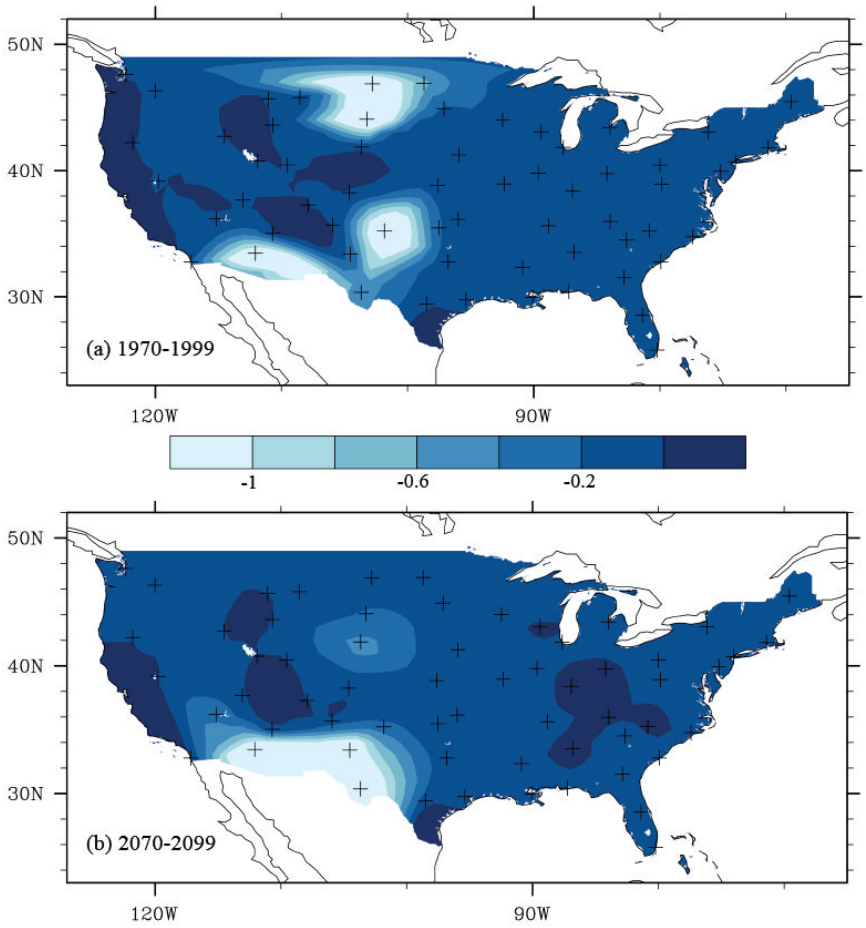

Fig. 6. As in Fig. 1, changes in precipitation water content (g m^{-3}) at the freezing level for a change in CCN from modest to polluted cases as described in text, for the past (a) and future (b) atmospheric profiles at the 61 sites for which the microphysical model was run (denoted by crosses).

4. Summary and Discussion

Differences in warm rain production in past and future convective clouds over different regions of the U.S. were investigated with a warm rain microphysical parcel model, using representative estimates of the local CCN along with past and future thermodynamic profiles derived from a single run with the NCAR CCSM3. By modeling the warm rain process in detail here, with physically plausible future atmospheric environments, the hypothesis that a warmer climate will lead to a more robust warm rain process has been tested, and refuted. The results indicate that:

- A warmer future climate may indeed enhance warm rain formation regionally, due to warmer, lower cloud bases and a greater depth from cloud base to the freezing level, but other factors may limit this enhancement, including: (i) the aridity of the region which may still yield a cloud base that is too high and thus limits the depth to the FL over which the warm rain process can act; (ii) an increased updraft speed beneath the FL that can limit the time for warm rain production; and (iii) too many CCN in the local environment.
- Some future environments may be so favorable for the warm rain process that they exhibit a decreased sensitivity to the number and characteristics of CCN ingested by the cloud, as in the Midwestern U.S. in this particular climate simulation.

- Regions where warm rain production has been marginal in the past, like the Western U.S., may see the greatest increases in a future warmer climate, particularly where boundary layer moisture is not lacking, but more time/depth between cloud base and the FL is needed for warm rain formation.

Although these results were derived from a single GCM simulation that exhibited a dry bias in the lower atmosphere, they demonstrate trends that can be used to interpret other climate scenarios, observed or simulated. Recently, Diffenbaugh et al. (2013) performed a statistical analysis of CAPE for an ensemble of GCMs, and found the same trends in CAPE as demonstrated in the CCSM3 results used here. Hence, the magnitudes of warm rain production at the FL found here may vary when compared to other studies due to differences in cloud base heights, but the same physical relationships demonstrated here with respect to the warm rain process and environmental factors that may enhance or mitigate it should remain valid.

This study is the first step needed to investigate the series of microphysical events that may lead to differences in extreme convective rainfall due to climate change. It highlights the need to consider not only the potential increase in cloud depth below the freezing level due to atmospheric warming, but also the effect that warming has on the updraft speed and how the local arid conditions or high aerosol concentrations can mitigate potential enhancements to the warm rain process. In more dynamically complex 3D models containing a simpler treatment of the warm rain process, for example those based only on the liquid water content of the cloud (e.g. Kessler, 1969), it suggests that care must be taken to ensure the parameterization properly addresses these mitigating factors. The Lagrangian parcel model used here is a simplification of the overall 3D dynamics of a real storm, but with the large amount of buoyancy in the soundings it should provide a realistic estimate within the core of a storm. A more sophisticated dynamical model must be used to test this assumption, and also to investigate how the warm rain process will interact with ice above the freezing level. Simulations using the Weather Research and Forecasting (WRF) model to address the interplay between the warm rain process and ice processes, and their overall effect upon convective rainfall in a changing climate, are currently underway. The parameterized warm rain development is being evaluated against the detailed warm rain calculations presented in the current study, to ensure the parameterization does not compromise its accuracy. These activities will be reported in a future paper.

Acknowledgements

Some microphysical model runs and analyses were conducted by members of the Purdue undergraduate course *Introduction to Atmospheric Science Research* offered in 2009 and 2010 and guided by Ms. Kathleen Quardokus as part of NSF award DUE-0837272. Conference presentations of earlier phases of this work by the first author were co-supported by travel awards from the EAS Department at Purdue University and the Purdue Climate Change Research Center. This is Purdue Climate Change Research Center paper #1216.

References

Allan, R. P., & Soden, B. J. (2008). Atmospheric warming and the amplification of precipitation extremes. *Science*, 321, 1481–1494. doi: 10.1126/science.1160787

Auer, A. H., Jr., (1975). The production of cloud and Aitken nuclei by the St. Louis metropolitan area (Project METROMEX). *J. Rech. Atmos.*, 9, 11–22.

Baeck, M. L., & Smith, J. A. (1998). Rainfall estimation by the WSR-88D for heavy rainfall events. *Wea.*

Forecasting, 13, 416–436. http://dx.doi.org/10.1175/1520-0434(1998)013<0416:REBTWF>2.0.CO;2

Berg, P., Moseley C., & Haerter J. O. (2013). Strong increase in convective precipitation in response to higher temperatures. *Nature Geoscience*, 6, 181–185. doi:10.1038/ngeo1731

Bluestein, H. B., McCaul E. W., Byrd G. P., Woodall G. R. (1988) Mobile Sounding Observations of a Tornadic Storm near the Dryline: The Canadian, Texas Storm of 7 May 1986. *Mon. Wea. Rev.*, 116, 1790–1804. http://dx.doi.org/10.1175/1520-0493(1988)116<1790:MSOOAT>2.0.CO;2

Braham, R. R., Jr. (1974). Cloud physics of urban weather modification—A preliminary report. *Bull. Amer. Meteor. Soc.*, 55, 100–106.

Brooks, H. E., Lee J. W., & Craven J. P. (2003). The spatial distribution of severe thunderstorm and tornado environments from global reanalysis data. *Atmos. Res.*, 67-68, 73-94. doi:10.1016/S0169-8095(03)00045-0

Caracena, F., Maddox R. A., Hoxit L. R., & Chappell C. F. (1979). Mesoanalysis of the Big Thompson Storm. *Mon. Wea. Rev.*, 107, 1–17. http://dx.doi.org/10.1175/1520-0493(1979)107<0001:MOTBTS>2.0.CO;2

Cash, J. R., & Karp A. H. (1990). A variable order Runge–Kutta method for initial value problems with rapidly varying right-hand sides. *ACM Transactions on Mathematical Software*, 16, 201–222. doi:10.1145/79505.79507

Cooper, W. A., Bruintjes R. T., & Mather G. K. (1997). Calculations pertaining to hygroscopic seeding with flares. *J. Appl. Meteor*., 36, 1449-1469. http://dx.doi.org/10.1175/1520-0450(1997)036<1449:CPTHSW>2.0.CO;2

Diffenbaugh, N. S., Scherer M., & Trapp R. J. (2013). Robust increases in severe thunderstorm environments in response to greenhouse forcing. *Proc. Nat. Acad. Sci.,* 110, 16361–16366 doi: 10.1073/pnas.1307758110

Freud, E., & Rosenfeld, D. (2012). Linear relation between convective cloud drop number concentration and depth for rain initiation, *J. Geophys. Res.*, 117, D02207. doi: 10.1029/2011JD016457

Frisbie, P. R., & Hudson, J. G. (1993). Urban cloud condensation nuclei spectral flux. *J. Appl. Meteor.*, 32, 666–676. http://dx.doi.org/10.1175/1520-0450(1993)032<0666:UCCNSF>2.0.CO;2

Fukuta, N., & Walter, L. A. (1970). Kinetics of hydrometeor growth from a vapor–spherical model. *J. Atmos. Sci.*, 27,1160–1172. http://dx.doi.org/10.1175/1520-0469(1970)027<1160:KOHGFA>2.0.CO;2

Golding, B. W., Clark P., & May B. (2005). The Boscastle flood: Meteorological analysis of the conditions leading to flooding on 16th August 2004. *Weather*, 60, 230–235. doi: 10.1256/wea.71.05

Heymsfield, A. J., Johnson D. N., & Dye J. E. (1978). Dye observations of moist adiabatic ascent in northeast Colorado cumulus congestus clouds *J. Atmos. Sci.*, 35, 1689–1703. http://dx.doi.org/10.1175/1520-0469(1978)035<1689:OOMAAI>2.0.CO;2

Hobbs, P. V., Politovich M. K., Bowdle D. A., & Radke L. F. (1978). *Airborne studies of atmospheric aerosol in the High Plains and the structures of natural and artificially seeded clouds in eastern Montana*. Cloud Physics Group Research Rep. 13, University of Washington.

_____, Bowdle D. A., & Radke L. F. (1985). Particles in the lower troposphere over the high plains of the United States. Part I: Size distributions, elemental composition, and morphologies. *J. Climate Appl. Meteor.*, 24, 1344–1356. http://dx.doi.org/10.1175/1520-0450(1985)024<1344:PITLTO>2.0.CO;2

Houze, R. A. (1977). Structure and dynamics of a tropical squall–line system. *Mon. Wea. Rev.*, 105, 1540–1567. http://dx.doi.org/10.1175/1520-0493(1977)105<1540:SADOAT>2.0.CO;2

Hudson, J. G., & Yum S. S. (2001). Maritime–continental drizzle contrasts in small cumuli. *J. Atmos. Sci.*, 58, 915–926. http://dx.doi.org/10.1175/1520-0469(2001)058<0915:MCDCIS>2.0.CO;2

Johnson, D. B. (1980). The influence of cloud base temperature and pressure on droplet concentration. *J. Atmos. Sci.*, 37, 2079-2085. http://dx.doi.org/10.1175/1520-0469(1980)037<2079:TIOCBT>2.0.CO;2

Junge, C. E., Robinson E., & Ludwig F. L. (1969). A study of aerosols in Pacific air masses. *J. Appl. Meteorol*, 8, 340–347. http://dx.doi.org/10.1175/1520-0450(1969)008<0340:ASOAIP>2.0.CO;2

Kalnay, E., & co-authors (1996). The NCEP/NCAR 40-year reanalysis project. *Bull. Amer. Meteor. Soc.*, 77, 437-471. http://dx.doi.org/10.1175/1520-0477(1996)077<0437:TNYRP>2.0.CO;2

Karl, T. R., & Knight R. W. (1998). Secular trends of precipitation amount, frequency, and intensity in the United States. *Bull. Amer. Meteor. Soc.*, 79, 231–241. http://dx.doi.org/10.1175/1520-0477(1998)079<0231:STOPAF>2.0.CO;2

Kessler, E. (1969). *On the distribution and continuity of water substance in atmospheric circulation*. Meteorological Monographs 10, 84.

Konwar, M., Maheskumar R. S., Kulkarni J. R., Freud E., Goswami B. N., & Rosenfeld D. (2012). Aerosol control on depth of warm rain in convective clouds, *J. Geophys. Res.*, 117, D13204. doi: 10.1029/2012JD017585

Kovetz, A., & Olund, B. (1969). The effect of coalescence and condensation on rain formation in a cloud of finite vertical extent. *J. Atmos. Sci.* 26, 1060 -1065. http://dx.doi.org/10.1175/1520-0469(1969)026<1060:TEOCAC>2.0.CO;2

Lasher-Trapp, S. G., Anderson-Bereznicki S., Shackelford A., Twohy C. H., & Hudson J. G. (2008). An investigation of the influence of droplet number concentration and giant aerosol particles upon supercooled large drop formation in wintertime stratiform clouds. *J. Appl. Meteor. Climatol.*, 47, 2659–2678. http://dx.doi.org/10.1175/2008JAMC1807.1

Lau, K. M., & Wu H. T. (2007). Detecting trends in tropical rainfall characteristics, 1979–2003. *Int. J. Climatol.*, 27, 979–988. doi: 10.1002/joc.1454

_____, _____ (2011). Climatology and changes in tropical oceanic rainfall characteristics inferred from Tropical Rainfall Measuring Mission (TRMM) data (1998–2009), *J. Geophys. Res.*, 116, D17111. doi: 10.1029/2011JD015827

Lindzen, R. S., Chour M.-D., & Hou A. Y. (2001). Does the earth have an adaptive infrared iris? *Bull. Amer. Meteor. Soc.*, 82, 417-432. http://dx.doi.org/10.1175/1520-0477(2001)082<0417:DTEHAA>2.3.CO;2

Maheshwari, R. C., & Mathur I. C. (1968). Radar reflectivity studies of Indian Summer Monsoon over Norhtwest India. *Preprints 13th Radar Meteorology Conf.*, Montreal, Amer. Meteor. Soc., 98-103.

Mesinger, F., & co-authors (2006). North American Regional Reanalysis. *Bull. Amer. Meteor. Soc.*, 87, 343–360. http://dx.doi.org/10.1175/BAMS-87-3-343

Musil, D. J., Heymsfield A. J., Smith P. L. (1986). Microphysical Characteristics of a Well-Developed Weak Echo Region in a High Plains Supercell Thunderstorm. *J. Climate Appl. Meteor.*, 25, 1037–1051. http://dx.doi.org/10.1175/1520-0450(1986)025<1037:MCOAWD>2.0.CO;2

Petersen, W. A., Carey L. D., Rutledge S. A., Knievel J. C., Johnson R. H., Doesken N. J., McKee T. B., Vonder Haar T., & Weaver J. F. (1999). Mesoscale and radar observations of the Fort Collins flash flood of 28 July 1997. *Bull. Amer. Meteor. Soc.*, 80, 191–216. http://dx.doi.org/10.1175/1520-0477(1999)080<0191:MAROOT>2.0.CO;2

Pruppacher, H. R., & Klett J. D. (1997). *Microphysics of Clouds and Precipitation*, 2nd edition, Kluwer Academic Publishing, Dordrecht, pp. 954.

Spyers-Duran, P. (1974). Cloud condensation nuclei measurements and estimates of production rates in the St. Louis urban complex. Preprints, Fourth Conf. on Weather Modification, Ft. Lauderdale, FL, *Amer. Meteor. Soc.*, 390–395.

Storer, R. L., van den Heever S., & Stephens G. L. (2010). Modeling aerosol impacts on convective storms in different environments. *J. Atmos. Sci*., 67, 3904-3915. http://dx.doi.org/10.1175/2010JAS3363.1

Trapp, R. J., Diffenbaugh N. S., Brooks H. E., Bladwin M. E., Robinson E. D., & Pal J. S. (2007). Changes in severe thunderstorm environment frequency during the 21st century caused by anthropogenically enhanced global radiative forcing. *Proc. Nat. Acad. Sci.*, 104, 19719-19723. doi: 10.1073/pnas.0705494104

_____, _____, & Gluhovsky A. (2009). Transient response of severe thunderstorm forcing to elevated greenhouse gas concentrations. *Geophys. Res. Lett.*, 36, L01703. doi:10.1029/2008GL036203.

Trenberth, K. E., Dai A., Rasmussen R. M., & Parsons D. B. (2003). The changing character of precipitation. *Bull. Amer. Meteor. Soc.*, 84, 1205–1217. http://dx.doi.org/10.1175/BAMS-84-9-1205

Twomey, S. (1976). Computations of the absorption of solar radiation by clouds. *J. Atmos. Sci.* 33, 1087-1091. http://dx.doi.org/10.1175/1520-0469(1976)033<1087:COTAOS>2.0.CO;2

Twomey, S., & Wojciechowski T. A. (1969). Observations of the geographical variation of cloud nuclei, *J. Atmos. Sci.*, 26, 648 651. http://dx.doi.org/10.1175/1520-0469(1969)26<648:OOTGVO>2.0.CO;2